

Derivations for Locating Photon Emission Points Using Compton Imaging in GRETINA

Dr. Robert Crabbs
University of California, Berkeley

Dr. I-Yang Lee
Lawrence-Berkeley National Laboratory

Dr. Kai Vetter
Lawrence-Berkeley National Laboratory

January 10, 2022

Abstract

GRETA, the **Gamma-Ray Energy Tracking Array**, is an array of highly-segmented HPGe detectors designed to track γ -rays emitted in beam-physics experiments. Its high detection efficiency and state-of-the-art position resolution make it well-suited for imaging applications. In this paper, we derive the expressions for locating a photon emission point using Compton imaging. We also include expressions for corresponding uncertainty calculations.

1 Introduction

In a typical in-beam experiment, a projectile nucleus is accelerated to high energy and directed into a beam target. Nuclear reactions in the target produce recoil nuclei heading downstream. These recoil nuclei are often excited, and can emit one or more characteristic γ -ray photons somewhere downstream of the target. By locating the emission points of these photons, we can determine the lifetime of the excited recoil nuclei.

Compton imaging is one method by which we can locate photon emissions. [1] A γ -ray typically interacts several times in an HPGe detector before being fully-absorbed, resulting in a sequence of hits in the detector denoted \mathbf{X}_1 to \mathbf{X}_N . (Figure 1) However, we cannot directly measure the interaction sequence because the detector electronics are not fast enough to resolve the differences in timing. Instead, we use Compton sequencing to deduce the sequence. [2]

Once we have the interaction sequence, we can define a “Compton cone” from detected energy depositions and the locations of the first 2 interactions. Each cone shows the possible directions from which a photon came as it entered the detector, and is uniquely defined by its vertex \mathbf{X}_C , central axis $\hat{\mathbf{V}}_C$, and cosine of opening angle $\mu_C = \cos \theta_C$.

The intersections of these Compton cones with the recoil beam are the possible emission points of the photons. Note that a cone will intersect a beam at (up to) 2 points. In practice, our cones will intersect the beam at 2 distinct locations, or else not at all. Real-world detector position & energy resolution can cause errors in the locations, energy depositions, and sequence of interactions; such errors can significantly skew the resulting Compton

cones. The following sections describe the math behind finding an emission point, \mathbf{X}_0 .

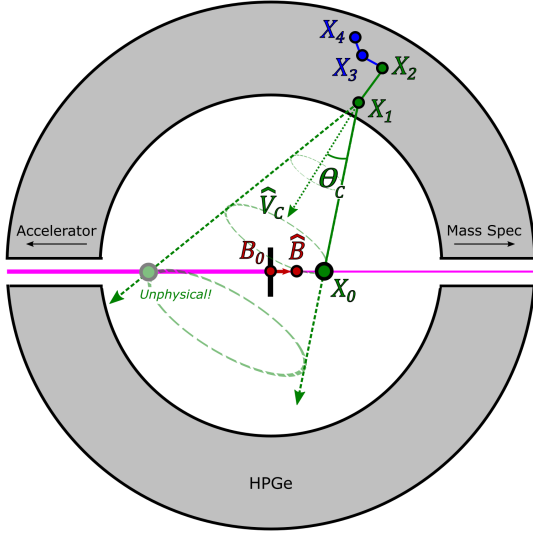


Figure 1: Geometry Used in Compton Imaging

2 Cone-Beam Intersections

Reference [3] provides a general geometric expression for the intersections between cones & beams, which we can adapt here for our specific problem. We seek an emission point \mathbf{X}_0 somewhere on the beam. Let's start by parametrizing our recoil beam as $\mathbf{B}(t) = \mathbf{B}_0 + \hat{\mathbf{B}}t$, with beam axis $\hat{\mathbf{B}}$ and beam anchor point \mathbf{B}_0 . In GRETINA or GRETA, the beamline lies along the $\hat{\mathbf{z}}$ -axis and passes through the origin of the lab frame, so we can simply set $\mathbf{B}_0 = (0, 0, 0)$ and $\hat{\mathbf{B}} = (0, 0, 1)$. This simplifies our expression for the emission point to $\mathbf{X}_0 = \mathbf{B}(t) = \hat{\mathbf{B}}t$.

As noted in Section 1, a Compton cone is defined by its vertex \mathbf{X}_C , central axis $\hat{\mathbf{V}}_C$, and cosine of opening angle $\mu_C = \cos \theta_C$. Our emission point \mathbf{X}_0 must also lie somewhere on this cone, which is true if:

$$\hat{\mathbf{V}}_C \cdot \frac{(\mathbf{X}_0 - \mathbf{X}_C)}{\|\mathbf{X}_0 - \mathbf{X}_C\|} = \mu_C \quad (1)$$

Re-arranging terms, we can rewrite this equation as:

$$\hat{\mathbf{V}}_C \cdot (\mathbf{X}_0 - \mathbf{X}_C) = \mu_C \|\mathbf{X}_0 - \mathbf{X}_C\| \quad (2)$$

Squaring both sides, we get:

$$(\hat{\mathbf{V}}_C \cdot (\mathbf{X}_0 - \mathbf{X}_C))^2 = \mu_C^2 \|\mathbf{X}_0 - \mathbf{X}_C\|^2 \quad (3)$$

Using the vector identities $(\mathbf{a} \cdot (\mathbf{b} - \mathbf{c}))^2 = (\mathbf{b} - \mathbf{c})^T \mathbf{a} \mathbf{a}^T (\mathbf{b} - \mathbf{c})$ and $(\mathbf{b} - \mathbf{c})^T (\mathbf{b} - \mathbf{c}) = \|\mathbf{b} - \mathbf{c}\|^2$, the above becomes:

$$(\mathbf{X}_0 - \mathbf{X}_C)^T \hat{\mathbf{V}}_C \hat{\mathbf{V}}_C^T (\mathbf{X}_0 - \mathbf{X}_C) = \mu_C^2 (\mathbf{X}_0 - \mathbf{X}_C)^T (\mathbf{X}_0 - \mathbf{X}_C) \quad (4)$$

$$(\mathbf{X}_0 - \mathbf{X}_C)^T M (\mathbf{X}_0 - \mathbf{X}_C) = 0 \quad (5)$$

where $M = \hat{\mathbf{V}}_C \hat{\mathbf{V}}_C^T - \mu_C^2 I_3$ is a 3×3 symmetric matrix. Substituting $\mathbf{X}_0(t) = \hat{\mathbf{B}}t$ in Equation 5, we get:

$$(\hat{\mathbf{B}}t - \mathbf{X}_C)^T M (\hat{\mathbf{B}}t - \mathbf{X}_C) = 0 \quad (6)$$

$$\hat{\mathbf{B}}^T M \hat{\mathbf{B}}t^2 - (\hat{\mathbf{B}}^T M \mathbf{X}_C - \mathbf{X}_C^T M \hat{\mathbf{B}})t + \mathbf{X}_C^T M \mathbf{X}_C = 0 \quad (7)$$

We can simplify this expression with the matrix identity $(DEF)^T = F^T E^T D^T$, noting that:

$$(\mathbf{X}_C^T M \hat{\mathbf{B}})^T = \hat{\mathbf{B}}^T M^T \mathbf{X}_C = \hat{\mathbf{B}}^T M \mathbf{X}_C \quad (8)$$

because M is symmetric. Since M is a 3×3 matrix, we know \mathbf{X}_C is a 3×1 column vector and $\hat{\mathbf{B}}^T$ is a 1×3 row vector. Therefore, $\hat{\mathbf{B}}^T M \mathbf{X}_C$ and $\mathbf{X}_C^T M \hat{\mathbf{B}}$ are both 1×1 scalars, and transposing them makes no difference. Therefore we can say that:

$$\hat{\mathbf{B}}^T M \mathbf{X}_C = (\mathbf{X}_C^T M \hat{\mathbf{B}})^T \quad (9)$$

$$= \mathbf{X}_C^T M \hat{\mathbf{B}} \quad (10)$$

This fact lets us rewrite Equation 7 as a quadratic equation in t :

$$\hat{\mathbf{B}}^T M \hat{\mathbf{B}} t^2 - 2\hat{\mathbf{B}}^T M \mathbf{X}_C t + \mathbf{X}_C^T M \mathbf{X}_C = 0 \quad (11)$$

Let $a = \hat{\mathbf{B}}^T M \hat{\mathbf{B}} = \hat{\mathbf{B}} \cdot (M \hat{\mathbf{B}})$, $b = -2\hat{\mathbf{B}}^T M \mathbf{X}_C = -2\hat{\mathbf{B}} \cdot (M \mathbf{X}_C)$, and $c = \mathbf{X}_C^T M \mathbf{X}_C = \mathbf{X}_C \cdot (M \mathbf{X}_C)$, so $at^2 + bt + c = 0$. This can be readily solved for t , and from there the cone-beam intersections are given by $\mathbf{X}_{0,1} = t_1 \hat{\mathbf{B}}$ and $\mathbf{X}_{0,2} = t_2 \hat{\mathbf{B}}$.

As mentioned before, when using imperfect detectors a Compton cone may not intersect the beamline at all. This is the situation when $b^2 - 4ac < 0$.

3 Error Propagation

We can compute analytical error estimates to judge the reliability of the reconstruction for an individual photon track. The full derivation contains 20 pages of partial derivatives – those have been omitted and “left as an exercise to the reader”.

Recall the general error propagation formula for a dependent variable z :

$$\sigma_z^2 = \sum_{j=1}^N \left(\frac{\partial z}{\partial x_j} \right)^2 \sigma_{x_j}^2 \quad (12)$$

where (x_1, \dots, x_N) are the independent variables from which z is calculated.

In Compton imaging, it might appear that we would only need 3 such variables to define a Compton cone: a vertex, an axis, and an opening angle. However, these 3 variables actually correspond to 8 independent variables. The cone’s vertex is the first hit in the photon track: $\mathbf{X}_C = \mathbf{X}_1 = (x_1, x_2, x_3)$. With the second photon hit at $\mathbf{X}_2 = (x_4, x_5, x_6)$, the cone axis is defined:

$$\hat{\mathbf{V}}_C = (v_1, v_2, v_3) \quad (13)$$

$$= \frac{\mathbf{X}_1 - \mathbf{X}_2}{\|\mathbf{X}_1 - \mathbf{X}_2\|} \quad (14)$$

$$= \left(\frac{x_1 - x_4}{L}, \frac{x_2 - x_5}{L}, \frac{x_3 - x_6}{L} \right) \quad (15)$$

where $L = \sqrt{(x_1 - x_4)^2 + (x_2 - x_5)^2 + (x_3 - x_6)^2}$ is the Compton “lever arm”. Lastly, the cone angle is determined by:

$$\mu_C = 1 - m_e c^2 \left(\frac{1}{E_1} - \frac{1}{E_0} \right) \quad (16)$$

where E_0 is the photon’s lab-frame emission energy and E_1 is the energy after the initial scatter in the detector. In all, we therefore need to measure 8 independent quantities to obtain a Compton reconstruction: $(x_1, x_2, x_3, x_4, x_5, x_6, E_0, E_1)$.

Note that in a real-world experiment, $\hat{\mathbf{B}}$ and \mathbf{B}_0 are not constant. Finite beam spot sizes and straggling can cause minor variations in the energies and directions of recoil nuclei. To account for such variations in

the recoil beam, then, we would also have to add the photon *parent's* trajectory to the list of independent variables. The velocity component is 4 variables: $\beta\hat{\mathbf{B}} = (\beta b_1, \beta b_2, \beta b_3)$, where $\hat{\mathbf{B}}$ is the heading for a particular recoil nucleus and βc is its speed. We would also need a beam setpoint, $\mathbf{B}_0 = (b_{0,1}, b_{0,2}, b_{0,3})$ that the recoil nucleus passes through. In all, this would add another 7 independent variables to the analysis: $(b_1, b_2, b_3, b_{0,1}, b_{0,2}, b_{0,3}, \beta)$. For simplicity, though, and because the variations in the recoil beam are typically not large, we have chosen to ignore these variables here.

In Section 2 we went over the math behind finding emission points with Compton imaging. The goal was to calculate the t 's in $\mathbf{X}_0 = \mathbf{B}_0 + t\hat{\mathbf{B}}$. In the end, we arrived at a quadratic equation:

$$t = \frac{-b \pm \sqrt{b^2 - 4ac}}{2a} \quad (17)$$

$$a = \hat{\mathbf{B}} \cdot (M\hat{\mathbf{B}}) \quad (18)$$

$$b = -2\hat{\mathbf{B}} \cdot (M\mathbf{X}_C) \quad (19)$$

$$c = \mathbf{X}_C \cdot (M\mathbf{X}_C) \quad (20)$$

Again, $M = \hat{\mathbf{V}}_C \hat{\mathbf{V}}_C^T - \mu_C^2 I_3$ is a 3×3 symmetric matrix:

$$M = \begin{pmatrix} v_1^2 - \mu_C^2 & v_1 v_2 & v_1 v_3 \\ v_1 v_2 & v_2^2 - \mu_C^2 & v_2 v_3 \\ v_1 v_3 & v_2 v_3 & v_3^2 - \mu_C^2 \end{pmatrix} \quad (21)$$

To get scalar expressions for error analysis, we evaluate a , b , and c with known quantities for the beam:

$$\mathbf{B}_0 = (0, 0, 0) \quad \hat{\mathbf{B}} = (0, 0, 1) \quad (22)$$

The matrix algebra is straightforward, yielding the following:

$$a = v_3^2 - \mu_C^2 \quad (23)$$

$$b = -2[v_1 v_3 x_1 + v_2 v_3 x_2 + (v_3^2 - \mu_C^2)x_3] \quad (24)$$

$$c = x_1^2(v_1^2 - \mu_C^2) + x_2^2(v_2^2 - \mu_C^2) + x_3^2(v_3^2 - \mu_C^2) + 2(v_1 v_2 x_1 x_2 + v_1 v_3 x_1 x_3 + v_2 v_3 x_2 x_3) \quad (25)$$

Furthermore, note that $\mathbf{X}_0 = \mathbf{B}_0 + t\hat{\mathbf{B}} = (0, 0, t)$, so we can identify the emission point simply by its z -coordinate, $z = t$.

Now that we have these expressions, the partial derivatives of z with respect to the independent variables $(x_1, \dots, x_6, E_0, E_1)$ can be calculated using the chain rule:

$$\frac{\partial z(y_1, \dots, y_N)}{\partial x_j} = \sum_{n=1}^N \left(\frac{\partial z}{\partial y_n} \right) \left(\frac{\partial y_n}{\partial x_j} \right) \quad (26)$$

Here, z is a function of the variables $a(x_1, \dots, x_6, E_0, E_1)$, $b(x_1, \dots, x_6, E_0, E_1)$, and $c(x_1, \dots, x_6, E_0, E_1)$ from our earlier quadratic equation. So, for example:

$$\frac{\partial z}{\partial x_1} = \frac{\partial z}{\partial a} \frac{\partial a}{\partial x_1} + \frac{\partial z}{\partial b} \frac{\partial b}{\partial x_1} + \frac{\partial z}{\partial c} \frac{\partial c}{\partial x_1} \quad (27)$$

Calculating the partial derivatives is a lengthy ordeal, and so we'll just provide the results below. Note that the partial derivatives of z contain a \pm or \mp sign, which reflect the root chosen in Equation 17. This only works when Compton imaging yields a unique emission point for the photon.

Now that we have partial derivatives for z with respect to each of the independent variables, we are close to an analytic estimate of the total error. To avoid confusion, we will refer to this estimated imaging resolution as σ_{img} instead of σ_z . The next step is to get a measure of uncertainty for each of the independent variables. In practice, GRETINA's position & energy resolution are both energy-dependent. In addition, position resolution is not spherically-symmetric – GRETINA's modules give positions more precisely radially than

axially. For simplicity, we have assumed that (x_1, \dots, x_6) are all equally-affected by the detector's position resolution, σ_{xyz} , and E_0 and E_1 are equally-affected by the detector's energy resolution, σ_E . Typical values are $\sigma_{xyz} = 3.0$ mm and $\sigma_E = 2.0$ keV.

Summing everything together with the Chain Rule, we find:

$$\sigma_{img}^2 = \left[\left(\frac{\partial z}{\partial x_1} \right)^2 + \left(\frac{\partial z}{\partial x_2} \right)^2 + \left(\frac{\partial z}{\partial x_3} \right)^2 + \left(\frac{\partial z}{\partial x_4} \right)^2 + \left(\frac{\partial z}{\partial x_5} \right)^2 + \left(\frac{\partial z}{\partial x_6} \right)^2 \right] \sigma_{xyz}^2 + \left[\left(\frac{\partial z}{\partial E_0} \right)^2 + \left(\frac{\partial z}{\partial E_1} \right)^2 \right] \sigma_E^2 \quad (28)$$

$$= \sigma_{img,pos}^2 + \sigma_{img,energy}^2 \quad (29)$$

We have separated the resolution estimate into two components – one depending entirely on position resolution ($\sigma_{img,pos}$) and one only on energy resolution ($\sigma_{img,energy}$). For detector resolutions typical of GRETINA, $\sigma_{img,pos} \gg \sigma_{img,energy}$ in Compton imaging.

Partial Derivatives of z

$$\frac{\partial z}{\partial a} = \frac{b}{2a^2} \pm \frac{c - b^2/2a}{a\sqrt{b^2 - 4ac}} \quad (30)$$

$$\frac{\partial z}{\partial b} = \frac{-1 \pm b/\sqrt{b^2 - 4ac}}{2a} \quad (31)$$

$$\frac{\partial z}{\partial c} = \frac{\mp 1}{\sqrt{b^2 - 4ac}} \quad (32)$$

Partial Derivatives of a

$$\frac{\partial a}{\partial x_1} = -\frac{2v_1v_3^2}{L} \quad \frac{\partial a}{\partial x_4} = -\frac{\partial a}{\partial x_1} \quad (33)$$

$$\frac{\partial a}{\partial x_2} = -\frac{2v_2v_3^2}{L} \quad \frac{\partial a}{\partial x_5} = -\frac{\partial a}{\partial x_2} \quad (34)$$

$$\frac{\partial a}{\partial x_3} = \frac{2v_3(1 - v_3^2)}{L} \quad \frac{\partial a}{\partial x_6} = -\frac{\partial a}{\partial x_3} \quad (35)$$

$$\frac{\partial a}{\partial E_0} = \frac{2\mu m_e}{E_0^2} \quad \frac{\partial a}{\partial E_1} = -\frac{2\mu m_e}{E_1^2} \quad (36)$$

Partial Derivatives of b

$$\frac{\partial b}{\partial x_1} = \frac{2v_3(2v_1^2x_1 - 2x_1 + x_4) + 4v_1v_2v_3x_2}{L} - 2x_3 \frac{\partial a}{\partial x_1} \quad (37)$$

$$\frac{\partial b}{\partial x_2} = \frac{2v_3(2v_2^2x_2 - 2x_2 + x_5) + 4v_1v_2v_3x_1}{L} - 2x_3 \frac{\partial a}{\partial x_2} \quad (38)$$

$$\frac{\partial b}{\partial x_3} = \frac{2(2v_3^2 - 1)(v_1x_1 + v_2x_2)}{L} - 2(a + x_3 \frac{\partial a}{\partial x_1}) \quad (39)$$

$$\frac{\partial b}{\partial x_4} = -\frac{2v_3x_1(2v_1^2 - 1) - 4v_1v_2v_3x_2}{L} - 2x_3 \frac{\partial a}{\partial x_4} \quad (40)$$

$$\frac{\partial b}{\partial x_5} = -\frac{2v_3x_2(2v_2^2 - 1) - 4v_1v_2v_3x_1}{L} - 2x_3 \frac{\partial a}{\partial x_5} \quad (41)$$

$$\frac{\partial b}{\partial x_6} = -\frac{2(2v_3^2 - 1)(v_1x_1 + v_2x_2)}{L} - 2x_3 \frac{\partial a}{\partial x_6} \quad (42)$$

$$\frac{\partial b}{\partial E_0} = -2x_3 \frac{\partial a}{\partial E_0} \quad \frac{\partial b}{\partial E_1} = -2x_3 \frac{\partial a}{\partial E_1} \quad (43)$$

Partial Derivatives of c

$$\begin{aligned} \frac{\partial c}{\partial x_1} = & 2v_1x_1^2(1 - v_1^2)/L + 2v_1v_2x_2(1 - v_2x_2)/L - 4v_1v_2v_3x_2x_3/L \\ & + 2x_1(v_2x_2 + v_3x_3)(1 - 2v_1^2)/L + x_3^2 \frac{\partial a}{\partial x_1} + 2x_1(v_1^2 - \mu^2) + 2v_1v_3x_3 \end{aligned} \quad (44)$$

$$\begin{aligned} \frac{\partial c}{\partial x_2} = & 2v_2x_2^2(1 - v_2^2)/L + 2v_1v_2x_1(1 - v_1x_1)/L - 4v_1v_2v_3x_1x_3/L \\ & + 2x_2(v_1x_1 + v_3x_3)(1 - 2v_2^2)/L + x_3^2 \frac{\partial a}{\partial x_2} + 2x_2(v_2^2 - \mu^2) + 2v_2v_3x_3 \end{aligned} \quad (45)$$

$$\begin{aligned} \frac{\partial c}{\partial x_3} = & 2x_3(v_1x_1 + v_2x_2)(1 - 2v_3^2)/L - 2v_3(v_1^2x_1^2 + v_2^2x_2^2)/L - 4v_1v_2v_3x_1x_2/L \\ & + 2v_3(v_1x_1 + v_2x_2) + x_3^2 \frac{\partial a}{\partial x_3} + 2x_3a \end{aligned} \quad (46)$$

$$\begin{aligned} \frac{\partial c}{\partial x_4} = & -2v_1x_1^2(1 - v_1^2)/L + 2v_1v_2^2x_2^2/L + 4v_1v_2v_3x_2x_3/L \\ & - 2x_1(v_2x_2 + v_3x_3)(1 - 2v_1^2)/L + x_3^2 \frac{\partial a}{\partial x_4} \end{aligned} \quad (47)$$

$$\begin{aligned} \frac{\partial c}{\partial x_5} = & -2v_2x_2^2(1 - v_2^2)/L + 2v_2v_1^2x_1^2/L + 4v_1v_2v_3x_1x_3/L \\ & - 2x_2(v_1x_1 + v_3x_3)(1 - 2v_2^2)/L + x_3^2 \frac{\partial a}{\partial x_5} \end{aligned} \quad (48)$$

$$\begin{aligned} \frac{\partial c}{\partial x_6} = & -2x_3(v_1x_1 + v_2x_2)(1 - 2v_3^2)/L + 2v_3(v_1^2x_1^2 + v_2^2x_2^2)/L \\ & + 4v_1v_2v_3x_1x_2/L + x_3^2 \frac{\partial a}{\partial x_6} \end{aligned} \quad (49)$$

$$\frac{\partial c}{\partial E_0} = \frac{2\mu m_e}{E_0^2}(x_1^2 + x_2^2) + x_3^2 \frac{\partial a}{\partial E_0} \quad (50)$$

$$\frac{\partial c}{\partial E_1} = -\frac{2\mu m_e}{E_1^2}(x_1^2 + x_2^2) + x_3^2 \frac{\partial a}{\partial E_1} \quad (51)$$

As mentioned, the derivation of the above partial derivatives was a lengthy process. We did try Mathematica's procedural derivative-calculator, but the generated formulae were much less tractable – sometimes taking up a full page each. Still, we were able to double-check our work numerically. Inputting hypothetical values of x_1 and the other independent variables produced identical results for both sets of formulae.

We also performed an independent numerical check by tweaking each independent variable for the sample Compton reconstruction in Table 2 below. By introducing small changes in x_1 or another of the variables, one can obtain numerical derivatives to compare with the results of the analytical expressions above. We used 0.01 mm increments for positions and 0.025 keV increments for energies.

Hit	x (mm)	y (mm)	z (mm)	ΔE (keV)
#1	-81.4542	172.4690	-30.0678	288.4240
#2	-100.3864	193.4548	-49.6538	210.0868
#3	-101.4564	193.9505	-52.1735	474.4475
#4	-96.0459	197.7831	-44.1857	0.6924
#5	-95.9333	197.8570	-43.9780	199.5873

Table 1: Sample photon track used in error estimates
Hits: 5, Track Energy: 1173.238keV

Partial Derivative	Analytic Estimate	Numeric Estimate	Partial Derivative	Analytic Estimate	Numeric Estimate
$\partial z/\partial a$	-0.08191	-	$\partial\theta/\partial E_0$	0.000723	0.000720
$\partial z/\partial b$	0.02344	-	$\partial\theta/\partial E_1$	-0.001271	-0.001266
$\partial z/\partial c$	-0.00671	-	-	-	-
$\partial a/\partial x_1$	-0.01039	-0.01040	$\partial b/\partial x_1$	-4.0290	-4.0284
$\partial a/\partial x_2$	0.01152	0.01150	$\partial b/\partial x_2$	1.7436	1.7467
$\partial a/\partial x_3$	0.02238	0.02237	$\partial b/\partial x_3$	5.2351	5.2424
$\partial a/\partial x_4$	0.01039	0.01040	$\partial b/\partial x_4$	3.4018	3.4033
$\partial a/\partial x_5$	-0.01152	-0.01153	$\partial b/\partial x_5$	-1.0484	-1.0458
$\partial a/\partial x_6$	-0.02244	-0.02237	$\partial b/\partial x_6$	-4.4115	-4.4043
$\partial a/\partial E_0$	0.000637	0.000640	$\partial b/\partial E_0$	0.0383	0.0383
$\partial a/\partial E_1$	-0.001120	-0.001120	$\partial b/\partial E_1$	-0.0674	-0.0673
$\partial c/\partial x_1$	-167.46	-166.95	$\partial z/\partial x_1$	1.0295	1.0253
$\partial c/\partial x_2$	-734.68	-733.81	$\partial z/\partial x_2$	4.9671	4.9613
$\partial c/\partial x_3$	-780.21	-780.22	$\partial z/\partial x_3$	5.3535	5.3571
$\partial c/\partial x_4$	103.26	103.73	$\partial z/\partial x_4$	-0.6136	-0.6170
$\partial c/\partial x_5$	684.85	685.43	$\partial z/\partial x_5$	-4.6166	-4.6217
$\partial c/\partial x_6$	633.98	633.96	$\partial z/\partial x_6$	-4.3535	-4.3510
$\partial c/\partial E_0$	23.752	23.746	$\partial z/\partial E_0$	-0.1585	-0.1584
$\partial c/\partial E_1$	-41.761	-41.755	$\partial z/\partial E_1$	0.2786	0.2785

Table 2: Numerical check of Compton imaging error estimates

Partial Derivative	Units	Partial Derivative	Units	Partial Derivative	Units
$\partial a/\partial x_j$	mm ⁻¹	$\partial b/\partial x_j$	-	$\partial c/\partial x_j$	mm
$\partial a/\partial E_k$	keV ⁻¹	$\partial b/\partial E_k$	mm keV ⁻¹	$\partial c/\partial E_k$	mm ² keV ⁻¹
$\partial z/\partial a$	mm	$\partial z/\partial x_j$	-	$\partial\theta/\partial E_k$	rad keV ⁻¹
$\partial z/\partial b$	-	$\partial z/\partial E_k$	mm keV ⁻¹	-	-
$\partial z/\partial c$	mm ⁻¹	-	-	-	-

Table 3: Units for partial derivatives

The differences between the analytical and numerical results are generally within 0.5%. Using our validated formulae, it's clear that the position resolution error component $\sigma_{img,pos}$ dominates the total imaging error. Energy resolution only affects the Compton cone angle, and for this example we see $\sigma_\theta = 0.00292$ radians (0.168°). A final note – with (3.000 mm, 2.000 keV) detector resolution, both the analytic and numeric estimated errors for this sample track are 29.253 mm. This relatively small imaging error can be attributed to the track's relatively long Compton lever arm of 34.387 mm. Analytic errors in the hundreds (or even thousands) of mm have been observed for other tracks where \mathbf{X}_1 and \mathbf{X}_2 are closer together.

References

- [1] R. Crabbs and I. Lee and K. Vetter. *Using Compton Imaging to Locate Moving Gamma-Ray Sources in the GRETINA Detector*. [arXiv.org](https://arxiv.org/abs/2007.05000). Published 2020, Accessed 2020-07-05.
- [2] R. Crabbs and I. Lee and K. Vetter. *Simulations of Compton Sequencing Using GRETINA*. [ArXiv.org](https://arxiv.org/abs/2005.05000). Published 2020, Accessed 2020-05-20.
- [3] D. Eberly. *Intersection of a Line and a Cone*. <http://www.geometrictools.com/Documentation/IntersectionLineCone.pdf>. Published 2000, Accessed 2014-12-29.